



Translation initiation in bacterial polysomes through ribosome loading on a standby site on a highly translated mRNA

Irena Andreeva^a, Riccardo Belardinelli^a, and Marina V. Rodnina^{a,1}

^aDepartment of Physical Biochemistry, Max Planck Institute for Biophysical Chemistry, 37077 Göttingen, Germany

Edited by Peter B. Moore, Yale University, New Haven, CT, and approved March 22, 2018 (received for review October 14, 2017)

During translation, consecutive ribosomes load on an mRNA and form a polysome. The first ribosome binds to a single-stranded mRNA region and moves toward the start codon, unwinding potential mRNA structures on the way. In contrast, the following ribosomes can dock at the start codon only when the first ribosome has vacated the initiation site. Here we show that loading of the second ribosome on a natural 38-nt-long 5' untranslated region of *lpp* mRNA, which codes for the outer membrane lipoprotein from *Escherichia coli*, takes place before the leading ribosome has moved away from the start codon. The rapid formation of this standby complex depends on the presence of ribosomal proteins S1/S2 in the leading ribosome. The early recruitment of the second ribosome to the standby site before translation by the leading ribosome and the tight coupling between translation elongation by the first ribosome and the accommodation of the second ribosome can contribute to high translational efficiency of the *lpp* mRNA.

ribosome | translation initiation | polysome formation | translational efficiency | global fitting

Translation efficiency (TE), defined as the number of protein molecules produced from one given mRNA molecule, depends on several factors, such as the frequency with which ribosomes are loaded on the mRNA and initiate translation, the velocity of translation elongation, as well as the stability of the mRNA and the protein (1–3). TE can be very sensitive to variations in translation initiation, as rates of initiation differ by more than 100-fold (4–6). In bacterial cells the initiation efficiency of an mRNA is determined by the properties of the ribosome binding site (RBS) and is further attenuated by interactions of the translating ribosome with RNA-polymerase (7–9) and with neighboring ribosomes in a polysome (10, 11). While translation initiation on free mRNAs has been extensively studied, the mechanism of ribosome loading onto a densely packed polysome is unclear.

In exponentially growing *Escherichia coli* cells, 70% of the ribosomes are found in polysomes (12). Ribosomes can load onto the mRNA in intervals of 1–3 s (10). The average polysome-packing density is 1.3 ribosomes per 100 nucleotides (nt) of mRNA, which yields an average ribosome spacing of 77 nt (13), with examples ranging from one ribosome every 72 nt on *luc* mRNA (14) to one in every 100 nt on *lacZ* mRNA (10, 15). Such ribosome spacing is much less tight than the maximum packing of one ribosome every 30 nt expected from the size of the ribosome footprint on mRNA. Computer modeling suggests that ribosome collisions and queues reduce translation efficiency substantially (10), which may explain a preference for moderate ribosome density. In some cases, polysome packing is very loose, such as on a galactoside acetyltransferase mRNA, which is loaded at 16-s intervals to result in a spacing of 580 nucleotides between consecutive ribosomes (16). In the cellular context such loose packing resembles ribosome binding to free mRNA or mRNA recruitment of the first (leading) ribosome during polysome formation. Translation by the leading ribosome can change the initiation efficiency of the following ribosomes in two ways. If the 5' untranslated region (5'UTR) of the mRNA contains secondary structures, and if refolding of these structures is slow

compared with RBS clearance by the translating ribosome, recruitment of the following ribosome may be facilitated by an increased accessibility of the RBS. This is referred to as ribosome drafting (17). On the other hand, the leading ribosome can slow down recruitment of the following ribosomes by occupying the RBS. Thus, the rate of ribosome loading on an mRNA may depend not only on the properties of the RBS, but also on the rate of translation at the beginning of the ORF (10, 18, 19). Such models imply different initiation kinetics for the leading and following ribosomes, but the experimental evidence for this notion is scarce.

Translation initiation on the leading ribosome entails three main steps. It begins with the formation of the 30S preinitiation complex (30S PIC), in which initiation factors (IFs) 1, 2, and 3, mRNA and initiator fMet-tRNA^{fMet} assemble on the small ribosomal subunit (30S) before start-codon recognition. Recruitment of mRNA to the 30S subunit is independent of IFs and fMet-tRNA^{fMet} (20, 21). The complementarity between the Shine-Dalgarno (SD) sequence in the mRNA and the anti-SD sequence in 16S rRNA places the start codon in the P site of the 30S subunit. However, if an mRNA forms secondary structures in the 5' UTR that mask the start codon and SD sequence, the 30S subunit can bind at a single-stranded region of the mRNA and then search along the mRNA for the initiation codon when the mRNA structure unwinds (21–24). Folded 5'UTRs bind to the platform region of the 30S subunit in the vicinity of ribosomal protein S2 (25). Protein S1, which is assembled onto protein S2, also contributes to the recruitment of such mRNAs and to the RNA-unwinding activity of the ribosome during initiation (26). Unwinding

Significance

Polysomes are ensembles of two or more consecutive ribosomes that translate mRNA into proteins. Adjacent ribosomes can affect the frequency with which a new ribosome is loaded into the polysome. Here we show that mRNA with a long 5'UTR can recruit the next ribosome when the genuine start site is still occupied by the leading ribosome. The second ribosome binds to the upstream standby site on the mRNA, helped by the ribosomal proteins S1/S2 of the preceding ribosome. When the translating ribosome has cleared the start codon, the consecutive ribosome can rapidly move to the translation start. Recruitment to the standby site is a mechanism to increase polysome density and to regulate the efficiency of translation in polysomes.

Author contributions: I.A., R.B., and M.V.R. designed research; I.A. and R.B. performed research; I.A. and R.B. analyzed data; and I.A., R.B., and M.V.R. wrote the paper.

The authors declare no conflict of interest.

This article is a PNAS Direct Submission.

This open access article is distributed under [Creative Commons Attribution-NonCommercial-NoDerivatives License 4.0 \(CC BY-NC-ND\)](https://creativecommons.org/licenses/by-nc-nd/4.0/).

¹To whom correspondence should be addressed. Email: rodnina@mpibpc.mpg.de.

This article contains supporting information online at www.pnas.org/lookup/suppl/doi:10.1073/pnas.1718029115/-DCSupplemental.

Published online April 9, 2018.

of secondary structures allows the mRNA to dock into the mRNA-binding channel of the 30S subunit. The anticodon of fMet-tRNA^{fMet} can then base-pair with the start codon, which converts the 30S PIC into the 30S IC. Subsequent joining of the large ribosomal subunit (50S) forms the 70S IC that can enter elongation (70S EC) (27).

Here we compare the initiation mechanisms employed by the leading and the following ribosomes in a fully reconstituted translation system from *E. coli*. As an example of an mRNA with high TE, we have chosen *lpp* mRNA, which codes for the major outer membrane prolipoprotein (Lpp, Braun's lipoprotein). Lpp is one of the most abundant proteins in *E. coli* and other Gram-negative bacteria (28, 29). It is essential for the stabilization of the cell wall and is a potent inducer of inflammation accompanying bacterial infections (30). Mutant strains where Lpp production is reduced do not grow and do not divide normally (31). The *lpp* gene is constitutively transcribed, and the mRNA is rather stable (half-life ~ 10 min in vivo) (32). Lpp is synthesized in 750,000 copies per cell, with a TE of 2.27 (28, 29). Such a high TE value is found also for EF-Tu (700,000 copies and TE of 2.29), one of the most abundant proteins in *E. coli*, and is much higher than that of other well-expressed proteins, such as ribosomal proteins or other translation factors (which have TE values of about 0.7). The high TE suggests that *lpp* mRNA can be efficiently loaded by consecutive ribosomes to form a polysome, but the mechanistic basis of the efficient ribosome recruitment is not known. In the present work we show that polysome loading on *lpp* mRNA proceeds via a standby site on the mRNA, which is distinct from the start-codon/SD sequence, and requires the interaction with ribosomal proteins S1/S2.

Results

Standby Site in Polysome Loading. The 5'UTR of the *lpp* mRNA is 38 nt in length (Fig. 1A) and is predicted to contain weak secondary structure elements with a folding energy of about -4 kcal/mol (SI Appendix, Fig. S1A). The native ORF codes for a 78 amino acid (aa)-long protein followed by a 50-nt-long 3'UTR (33). To test whether the 5'UTR of *lpp* contributes to its high TE, we used dual reporter luciferase assays (SI Appendix, Fig. S1B). We constructed expression plasmids carrying a T7 RNA-polymerase transcription site, the 5'UTR of interest followed by the Renilla luciferase (*rluc*) ORF, and a second 5'UTR from the pET24 vector followed by the Firefly luciferase (*fluc*) ORF. Transcription yields a polycistronic mRNA with a variable *rluc* and a constant *fluc* expression; the latter is used as an internal control for calculations. For quantitative comparison, we utilized the scale of 111 RBS constructs tested for their expression strength, which covers two orders of magnitude in expression levels (34). As an example of an RBS with a basal expression level we used *R0004* (34). Rluc expression is 12.6-fold higher with the *lpp* than with *R0004* 5'UTR (SI Appendix, Fig. S1C), which places the *lpp* leader among the 25% best on the scale of the tested RBS constructs (34) (SI Appendix, Fig. S1D).

Next, we developed an assay to monitor the 30S subunit binding to the mRNA in vitro. The fluorescence reporter group, Atto 488, was attached to the 5' end of the *lpp* RBS RNA primer. To limit the potential influence of the coding sequence both on the secondary structure of the 5'UTR and on the elongation rate, we replaced the native coding sequence with a poly(U) stretch of about 100 nt in length (Fig. 1A and SI Appendix, Fig. S1E and F) using primer extension by a template-independent poly(U)-polymerase (35); the resulting fluorescence-labeled mRNA is referred to as 5**lpp*. The functional activity of the mRNA in forming the 30S IC and 70S IC is demonstrated by nitrocellulose filtration and translation assays (SI Appendix, Fig. S1).

We first monitored the binding of the 5**lpp* mRNA to the 30S PIC [Fig. 1B, experiment (Exp. A)]. Upon binding, 5**lpp* fluorescence increases from the initial level—which we denote as F_0 —by 10% to the level that we refer to as F_1 , whereas no fluorescence change is observed in the absence of 30S subunits (Fig. 1B and SI Appendix, Fig. S2A). The fluorescence change is

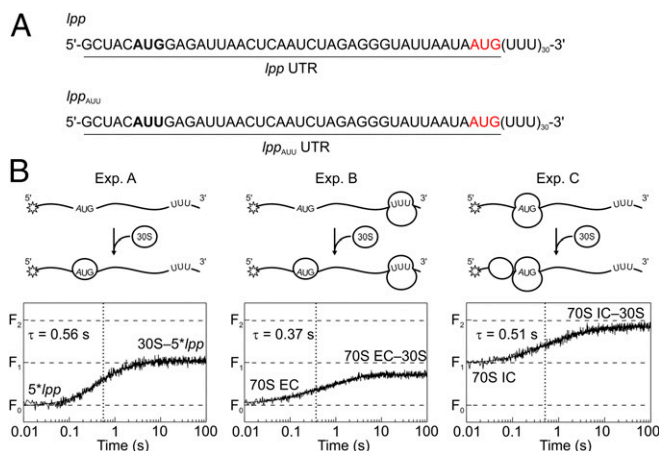


Fig. 1. Recruitment of the 30S PIC to 5**lpp* mRNA. (A) Sequences of the 5'UTR of *lpp* mRNA and the mutant *lpp*_{AUU} mRNA. The start codon of the ORF is shown in red, and an AUG codon at the mRNA 5' end is in bold. Underlined are the sequences of RNA primers used in the poly(U)-polymerase reaction. (B) Fluorescence change of 5**lpp* mRNA upon binding to the 30S PIC. Exp. A: Recruitment of 30S PIC to free 5**lpp* mRNA. A schematic of the reaction is shown in the cartoon. AUG is the start codon of the ORF; the rest of the coding region is replaced with a poly(U) sequence; "30S" denotes 30S PIC (0.3 μ M) formed of 30S subunits, IF1, IF2-GTP, and IF3. The initial fluorescence of free mRNA is referred to as F_0 , and the final fluorescence is referred to as F_1 . Exp. B: Recruitment of the 30S PIC to 5**lpp* mRNA, which has been translated by the leading 70S ribosome. The 70S IC was formed on 5**lpp* (0.05 μ M), purified from initiation components and mixed with excess of EF-Tu, EF-G, Phe-tRNA, and GTP to initiate elongation. The 70S EC is stalled at the end of the poly(U) track. The liberated RBS recruits the second 30S PIC (0.3 μ M). Exp. C: Recruitment of the 30S PIC to the 70S IC occupying the start codon of 5**lpp* mRNA. The 70S IC was prepared as in Exp. B and mixed with the 30S PIC in the absence of the translation mixture. The starting fluorescence F_1 is due to the binding of the first ribosome (Exp. A). The fluorescence of 5**lpp* mRNA with two ribosomes bound to the 5'UTR is F_2 .

biphasic with a predominant rapid phase accounting for $\sim 2/3$ of the total fluorescence amplitude, followed by a slower phase. The apparent rate constant of the rapid phase, k_{app1} , increases linearly with ribosome concentration (SI Appendix, Fig. S2), suggesting that it represents a bimolecular binding step. The concentration dependence of the apparent rate constant of the slower step, k_{app2} , is hyperbolic, as expected for a conformational rearrangement following binding. The fluorescence change is very similar in the presence or absence of fMet-tRNA^{fMet} and is independent of the addition of the initiation factors or 50S subunit (SI Appendix, Figs. S2 and S3A). This suggests that the reporter monitors the initial steps of mRNA binding to the 30S subunit before start-codon recognition or 50S subunit joining. The rate constants of binding calculated from the concentration dependence of the k_{app} values are summarized in SI Appendix, Fig. S2C. At a given concentration of the 30S PIC, the overall kinetics of binding can be described by the characteristic recruitment time (τ) corresponding to the lifetime of the F_0 to F_1 transition, e.g., $\tau = 0.56$ s at 0.3 μ M 30S PIC (Fig. 1B and see SI Appendix, SI Materials and Methods). In the following, we will use the τ values to facilitate direct comparison between individual time courses.

Next, we sought to mimic the recruitment of the 30S PIC to the mRNA in the polysome. When the mRNA is translated, the leading ribosome moves along the mRNA and liberates the RBS for binding of the next ribosome (Fig. 1B, Exp. B). We formed the leading 70S IC and purified the complex from the initiation factors. Then, we started translation by adding elongation factors EF-Tu, EF-G, with GTP and Phe-tRNA^{Phe}. Translation resulted in the incorporation of about 30 phenylalanine residues into the nascent chain with an average rate of 2.8 aa⁻¹ (SI Appendix, Fig. S2F). Because the mRNA lacks a stop codon at the end of

the coding sequence, and the translation system does not contain any factors that could release the ribosome from the mRNA, the leading ribosome remains bound to the mRNA after translation is completed. Then, we rapidly mixed these 70S EC with the 30S PIC. The recruitment of the 30S PIC results in a fluorescence change from level F_0 to F_1 with $\tau = 0.37$ s (Exp. B), similar to the ribosome recruitment on the free mRNA (Exp. A). Thus, the mRNA recruitment rates of the leading and following ribosomes are similar, provided the RBS is accessible.

To test whether the 70S IC residing on the start codon prevents the recruitment of the following 30S PIC, we prepared the 70S IC as described above, but did not add the translation components (Fig. 1B, Exp. C). Surprisingly, fluorescence increased to a higher F_2 level, indicating that the 30S PIC is recruited to the part of the mRNA that is free from the leading ribosome, rather than to the start codon. When the F_2 level is reached, addition of excess 30S PIC does not change the fluorescence further (SI Appendix, Fig. S3B). The recruitment time τ is 0.51 s (Exp. C), similar to that observed when the start codon is free. The part of the 5'UTR that is not engaged by the leading 70S IC can form weak secondary structures, but the folding energy is even less favorable than that of the free 5'UTR (SI Appendix, Figs. S1A and S3C). Thus, the 5'UTR of *lpp* mRNA is capable of recruiting two ribosomes, a 70S IC that occupies the start codon and a 30S PIC that binds to the mRNA upstream of the start codon, the latter in a standby position waiting for the leading ribosome to vacate the start site.

The observed 30S PIC binding upstream of the regular start codon might be directed by the silent AUG codon located 6 nt from the mRNA 5' end and 30 nt upstream of the regular AUG. To test the role of the upstream AUG, we mutated it to AUU (Fig. 1A and SI Appendix, Fig. S1 F–H). The mutant *lpp*_{AUU} mRNA, either free or in complex with the 70S IC bound at the start codon, recruits the upstream 30S PIC almost as efficiently as the mRNA with the native AUG (SI Appendix, Fig. S4). The recruitment time of the 30S PIC is twofold longer than that with the WT sequence, but the final fluorescence is the same. This indicates that determinants in the 5'**lpp* mRNA other than the upstream AUG are responsible for the 30S PIC standby recruitment.

To test whether the second ribosome is recruited at the standby position of the natural *lpp* mRNA as well, we repeated the two key experiments A and C with the full-length mRNA transcript (5'**lpp*-fl; SI Appendix, Fig. S5A). Binding of the 5'**lpp*-fl mRNA to the 30S IC leads to a fluorescence increase, albeit the rate of the reaction is somewhat reduced compared with the construct with poly(U) as a coding sequence (SI Appendix, Fig. S5B). Addition of the 30S PIC to the 70S IC results in further increase of fluorescence indicating the recruitment to the mRNA of the second 30S subunit (SI Appendix, Fig. S5C). Thus, 30S subunit loading onto the standby site when the leading ribosome occupies the start codon occurs independently of the coding sequence of the mRNA.

Role of Ribosomal Proteins S1 and S2. Ribosomal proteins S1 and S2 have been implicated in standby interactions with structured mRNAs (23, 25, 26). To test whether these interactions play a role in initiation on 5'**lpp* mRNA, we used mutant ribosomes depleted of S1 and S2 (30S Δ or 70S Δ ; Fig. 2 and SI Appendix, Figs. S1K and S6). The 30S Δ IC (if formed) is not stable (SI Appendix, Fig. S1H), and the 5'**lpp* fluorescence does not change (SI Appendix, Fig. S6A). Formation of the stable 70S Δ IC (SI Appendix, Fig. S1I), translation (SI Appendix, Figs. S1J and S2F), and the recruitment of the WT 30S subunit concomitant to the translation by the 70S Δ EC do not result in a reliable fluorescence effect (SI Appendix, Fig. S6B and C). After the leading 70S Δ EC has translated the mRNA, recruitment of the WT 30S IC takes place in the normal way, i.e., the fluorescence increases from F_0 to F_1 independent of whether the first round of translation was carried out by the 70SWT or 70S Δ ribosomes (Fig. 2, Exp. BA). However, when the leading 70S Δ IC occupies the start

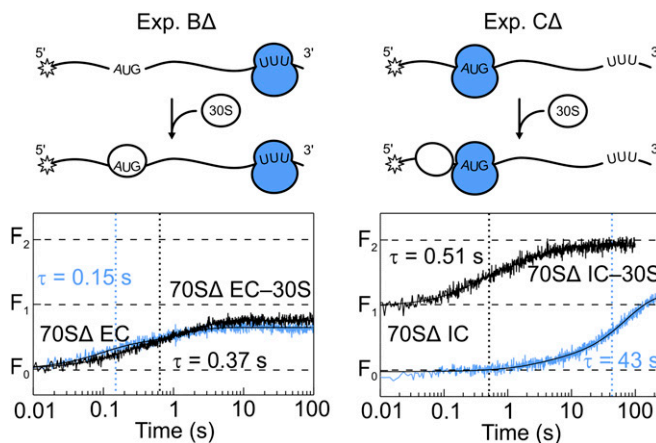


Fig. 2. The role of proteins S1/S2. Exp. BA: Recruitment of the 30S PIC to 5'**lpp* mRNA, which has been translated by the leading 70S Δ EC. Cartoon represents the schematic of the reaction as in Exp. B in Fig. 1, but performed with the leading ribosome lacking proteins S1 and S2 (shown blue in the cartoon). The 70S Δ IC was formed on 5'**lpp* mRNA (0.05 μ M) mixed with the excess of EF-Tu, EF-G, Phe-tRNA, and GTP to initiate elongation (70S Δ EC). After translation is completed, WT 30S PIC (0.3 μ M, white symbol in the cartoon) was added, and the fluorescence change upon recruitment to 5'**lpp* mRNA was monitored (blue trace; 70S Δ EC–30S). The analogous experiment with the WT 70S EC as a leading ribosome is shown for comparison (black trace). Exp. CA: Recruitment of the WT 30S PIC to 5'**lpp* mRNA when the start codon is occupied by the 70S Δ IC (blue trace) or WT 70S IC (black trace). Cartoon is the same as Exp. C in Fig. 1.

codon, recruitment of the 30S PIC to the standby site is very slow, with recruitment time of about 43 s compared with 0.51 s for the leading ribosome that contains S1 and S2 (Fig. 2, Exp. CA). Thus, S1/S2 are not only important for the initial recruitment of structured mRNAs on the given ribosome, but may also affect (by as much as 85-fold) the loading time of the following ribosome on the same mRNA.

Initiation on mRNA During Translation. Next, we studied binding of the 30S PIC to the 5'**lpp* mRNA that is being translated by the leading 70S ribosome. We first tested whether 5'**lpp* fluorescence changes during translation by the leading 70S EC (Fig. 3, Exp. D). When we add the elongation machinery to 70S IC, the 5'**lpp* fluorescence decreases from the F_1 level to the F_0 level, indicating the movement of the 70S EC away from the mRNA 5' end in the course of translation. The fluorescence decrease depends on the pace of elongation, i.e., in the absence of EF-G the fluorescence remains on the F_1 level, whereas at low EF-G concentrations the transition to the F_0 level occurs much more slowly than at saturating EF-G concentration (SI Appendix, Fig. S7A). Similarly, when translation is initiated in the complex with a leading 70S IC assembled on the start codon and a 30S PIC waiting in the standby position (Fig. 3, Exp. E), the starting fluorescence F_2 decreases to F_1 due to the 70S EC moving away from the initiation site upon translation. At the same time the 30S PIC likely moves from the standby site to the start codon, but the respective fluorescence change is hidden in the overall kinetics. Finally, when translation starts simultaneously with the addition of the 30S PIC (Fig. 3, Exp. F), initial fluorescence F_1 —which corresponds to the fluorescence of the 5'**lpp* mRNA bound to the 70S IC—first increases due to the recruitment of the following 30S PIC and then decreases when the translating 70S EC moves away from the 5' end of the mRNA. The final level F_1 is due to 30S IC assembly, as in Exp. B. The relative amplitudes of fluorescence increase and decrease depend on the rate of translation (SI Appendix, Fig. S7B). In the presence of EF-G in low concentrations, the intermediate with translating

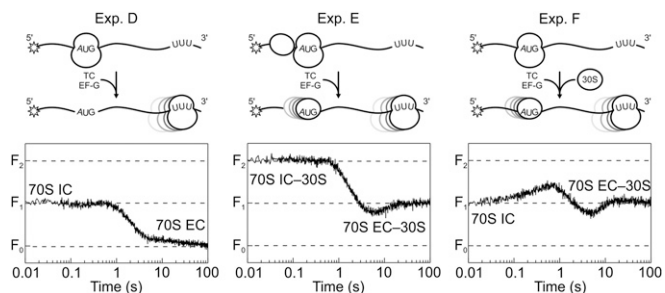


Fig. 3. The 30S PIC loading during mRNA translation by the leading ribosome. Exp. D: Fluorescence change of 5**lpp* mRNA upon translation by the leading 70S EC. The 70S IC (0.05 μM) was rapidly mixed with the translation mix [ternary complex (TC) and EF-G, with GTP]. Cartoon indicates movement of the leading 70S EC upon translation. Exp. E: Same as in Exp. D, but in the presence of the 30S PIC (0.4 μM) bound at the standby site. Cartoon indicates that the 30S PIC movement from the standby site toward the start codon (Fig. 4). Exp. F: Fluorescence of 5**lpp* mRNA upon addition of 30S PIC (0.4 μM) and the translation machinery to the purified 70S IC (0.05 μM). Cartoon indicates translation by the leading 70S EC and the movement of the 30S PIC from the standby site to the vacated start site.

70S EC and 30S PIC at the standby position accumulates because translation is slow and decreases back to the F_1 level more slowly than in the presence of saturating EF-G concentrations. Thus, while the leading ribosome translates the mRNA, the next 30S PIC is recruited to the standby site of the mRNA and then moves to the start codon vacated by the leading ribosome.

To dissect the kinetic mechanism of 30S PIC loading onto the mRNA while it is translated by the leading ribosome, we deconvoluted the 30S PIC binding and translation steps (Fig. 4A and *SI Appendix*, Fig. S8). To analyze the initial recruitment of the 30S PIC to the translating ribosome, we calculated the difference between Exps. E and F. The time course of Exp. F contains all of the information about the complete process of 30S PIC binding, including initial recruitment to the standby site followed by the accommodation at the vacated start codon. By contrast, in Exp. E the initial recruitment has already happened, and the time course reflects translation and the following 30S PIC rearrangement steps (*SI Appendix*, Fig. S8A). Thus, subtraction of trace E from F yields the fluorescence change associated with the initial recruitment of 30S PIC to the standby site before the accommodation at the start codon (Fig. 4B, *Left*). The resulting deconvoluted time course is biphasic, similarly to the two-step recruitment of the 30S PIC to free 5**lpp* mRNA (Fig. 1B, Exp. A, and *SI Appendix*, Fig. S2).

The difference trace between the time courses of Exps. E and D (Fig. 3) represents the fluorescence change associated with the 30S PIC accommodation at the start codon, while the initial recruitment of the 30S PIC is not monitored, and the fluorescence change due to translation is the same in E and D, such that the respective signal changes cancel out (Fig. 4B, *Middle*). The deconvolution reveals a biphasic kinetics, with a rearrangement resulting in a decrease of 5**lpp* fluorescence followed by a slower increase. Finally, the difference between Exp. F and D contains the complete information on the binding of the initial recruitment 30S PIC and the subsequent steps resulting in the accommodation at the start codon vacated by the leading 70S EC (Fig. 4B, *Right*). To validate the deconvolution approach, we compared recorded and calculated time courses obtained by deconvolution. For example, subtraction of Exp. C from Exp. F should yield the time course monitored in Exp. E (*SI Appendix*, Fig. S8A), which is indeed the case in this and other tested cases (*SI Appendix*, Fig. S8B and C).

We then used deconvoluted time courses for two 30S PIC concentrations (0.05 μM and 0.4 μM ; *SI Appendix*, Fig. S9) to obtain a global fit to a minimal four-step kinetic model (Fig. 4A), which includes two steps (steps 1 and 2) of the initial recruitment

to the standby site (Fig. 4B, *Left*) and two steps (steps 3 and 4) of the rearrangements ending with the accommodation at the start site (Fig. 4B, *Middle*). For simplicity, we assume that all steps are quasi-irreversible, reflecting the strong forward commitment toward the formation of the stable 30S IC. The calculated rates represent the overall speed of progression, although the underlying fluctuations are likely reversible. The global fitting resulted in rate constants for the model of Fig. 4A: $k_1 = 24 \pm 3 \mu\text{M}^{-1}\text{s}^{-1}$, $k_2 = 0.8 \pm 0.1 \text{ s}^{-1}$, $k_3 = 4 \pm 1 \text{ s}^{-1}$, and $k_4 = 0.15 \pm 0.03 \text{ s}^{-1}$. The rate constant of the initial recruitment during translation ($24 \mu\text{M}^{-1}\text{s}^{-1}$) is somewhat higher than the recruitment to the free mRNA ($5 \mu\text{M}^{-1}\text{s}^{-1}$), whereas the subsequent docking at the standby site has a similar rate in the two systems (0.8 and 0.6 s^{-1} , respectively). When translation starts, the complex undergoes a rapid rearrangement (4 s^{-1}), followed by the accommodation of the 30S IC (0.15 s^{-1}) limited by the rate of translation (0.10 s^{-1}) (Fig. 4B, *Right Bottom*). Thus, the polysome assembly on *lpp* mRNA is ensured by the early recruitment of the 30S PIC to the standby site, which takes place before translation by the leading ribosome begins, followed by rapid movement to the start codon as soon as the leading ribosome moves away.

Discussion

Our data suggest the following model for polysome assembly on the *lpp* mRNA (Fig. 5). After the formation of the leading 70S IC, the next 30S subunit can rapidly bind to the mRNA at a region upstream of the leading ribosome at a standby site. The 23 nt of the 5'UTR remaining for binding of the second ribosome when the first ribosome occupies the start codon is apparently sufficient to make the initial contact. The initial recruitment rate for the *lpp* mRNA ($24 \mu\text{M}^{-1}\text{s}^{-1}$) in the polysome is within the range of association rates reported for different mRNAs, from 6 to $250 \mu\text{M}^{-1}\text{s}^{-1}$ (20, 21). The second ribosome can be recruited faster than the first one ($5 \mu\text{M}^{-1}\text{s}^{-1}$), which may be explained by the decreased propensity of the accessible mRNA region to form secondary structures. Also similar for the leading and following ribosomes, the rearrangement step of 0.8 s^{-1} reflects a step of the mRNA docking on the standby site that precedes ribosome accommodation on the start codon. For the leading ribosome, we only monitor these two steps, whereas the following accommodation on the start codon is not monitored

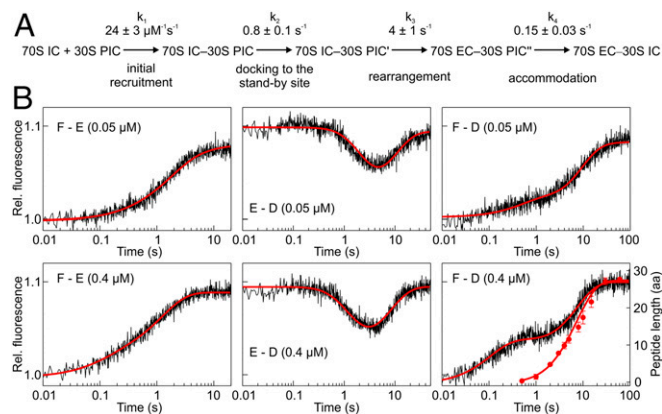


Fig. 4. Dissecting the initiation kinetics in a polysome. (A) A kinetic mechanism used for global fitting. Errors are SEM of the fit. (B) Deconvoluted time courses for the initial recruitment of the 30S PIC to the standby site (*Left*); of the rearrangement and accommodation at the start site (*Middle*); and of the overall reaction (*Right*). For 0.05 μM 30S PIC. (*Top*) For 0.4 μM 30S PIC. The experimental time courses used for deconvolution are indicated in each panel. The results of global fit are shown as red lines. Error bars for the translation elongation kinetics are SD ($n = 4$ independent experiments).

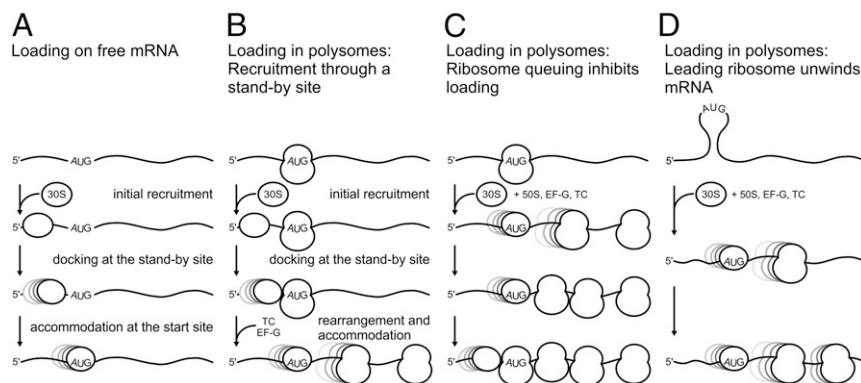


Fig. 5. Kinetic models of translation initiation. (A) Simplified model of translation initiation on a free mRNA. Initial recruitment is followed by the docking at the standby site. Subsequent accommodation at the start site forms the 30S IC, which after 50S docking can enter the elongation step. (B–D) Loading of the successive ribosomes into a polysome. (B) The second ribosome can bind and dock at the standby site before the leading ribosome moves away from the start codon. Translation is limiting the rate of the second initiation. (C) Queuing of ribosomes at the coding sequence due to, e.g., rare codons preventing loading of the following ribosomes, thereby decreasing the rate of initiation and the overall TE (10, 18, 19). (D) The leading ribosome helps to unwind folded mRNA. If refolding is slower than the start-codon clearance, the following ribosome can bind the mRNA in the polysome faster than the free mRNA (17).

directly. The previously reported accommodation rate for other mRNAs is 0.5 s^{-1} and limited by codon recognition (20, 36). Assuming a similar rate of codon–anticodon recognition for the *lpp* mRNA, the docking and codon-recognition steps together would cause a short delay (about 3 s) between the recruitment of the leading ribosome and the beginning of translation elongation.

For the following ribosome, the situation is different. Although the 30S PIC is rapidly recruited and can dock at the standby site, the following steps depend on translation elongation by the leading ribosome. We identify two additional initiation rearrangements manifested by rapid (4 s^{-1}) and slow (0.15 s^{-1}) steps. The origin of the rapid rearrangement step is unclear. Because it is observed only when the first ribosome starts translation, it could reflect a reaction related to the initial steps of elongation, e.g., the release of the SD–aSD interactions by the first ribosome, a conformational change of the mRNA, or a change in the interactions between the two adjacent ribosomes. The slowest step of initiation by the second ribosome coincides with the rate of translation by the first ribosome. This slow loading of the second ribosome on the start codon gives the first ribosome enough time to move by about 56 nt away from the start codon (calculated from the time of accommodation, $1/0.15 \text{ s}$, and the rate of translation, $2.8 \text{ aa}\cdot\text{s}^{-1}$). Within the precision of such calculations, this value is close to the average ribosome spacing of 77 nt between adjacent ribosomes. Given that in our experiments the 30S subunits are waiting for the leading ribosome to leave, and thus the polysome density depends solely on translation elongation, the observed ribosome packing may represent the optimum or even close-to-maximum attainable polysome density, which may be determined by the orientation of the ribosomes in a polysome (14) or the large-scale dynamics of the L1 and L12 stalks of the ribosome. In the natural setting, the rate of translation is defined by the coding sequence, and thus the polysome density is likely modulated by the elongation rate, but the propensity for efficient loading is the property of mRNA 5' UTR.

Early recruitment of ribosomes to the standby site and the tight coupling between initiation and elongation makes the elongation step rate-limiting for ribosome loading onto the polysome. Depending on the coding sequence of the mRNA this may have a profoundly different effect on initiation. When the rate of elongation is slow, e.g., due to the presence of rare codons at the beginning of the ORF, this can limit the frequency of ribosome loading (19). In contrast, for rapidly translating sequences, this may lead to increased loading and thus result in higher TE values. We note that similarly to the poly(U) sequence, which we used in the present experiments, the native

coding sequence of *lpp* mRNA does not contain rare codons (Codon Adaptation Index is 0.8) and should be translated rapidly (33). Thus, early ribosome recruitment to the standby site in combination with the tight coupling between translation elongation and ribosome accommodation at the start codon can explain the high TE of the *lpp* mRNA and may be a hallmark of polysome assembly for highly expressed mRNAs in general. Thus, the 30S subunit recruitment via the standby site provides yet another mechanism to regulate translation initiation in polysomes, in addition to codon usage, which defines how rapidly the first ribosome vacates the start site (19), and ribosome drafting, which regulates polysome formation on mRNAs that have a propensity to form slowly folding structures (17) (Fig. 5).

The standby initiation complex is a state distinct from the canonical 30S IC complex formed upon proper positioning of the AUG codon in the P site. We note that there are two definitions of the standby. In addition to the original notion of the standby site as an mRNA single-stranded region outside the start codon (21–24), the same term is operationally used to describe the part of the ribosome that helps recruiting mRNAs (25, 26), including those with extended secondary structures or weak SD sequences (25, 26). On the 30S subunit, the platform region involved in recruitment of such mRNAs comprises proteins S1, S2, S7, S11, S18, and S21 (25). Ribosome docking at the standby site could help to unwind the mRNA or trap some specific interactions that favor the subsequent accommodation of the mRNA on the 30S subunit (26). There are striking similarities between the *lpp* mRNA and the structured mRNAs that are recruited to the standby site: the binding is multiphasic and depends on the presence of proteins S1/S2, and the binding site on the mRNA is distinct from the canonical translation initiation site. Thus, the formation of an initial standby complex may be part of a general mechanism for recruiting structured and unstructured mRNAs alike. In addition to providing optimal ribosome loading in polysomes and unwinding of folded mRNAs, the interaction with the S1/S2 platform may protect the 5' UTR from premature degradation, thereby indirectly affecting TE.

One interesting observation is that when the leading ribosome lacks proteins S1/S2, recruitment of the following WT ribosome is delayed by as much as 85-fold. This suggests the existence of a yet unknown interplay between the adjacent ribosomes in the polysome mediated by S1/S2. Changes in the expression level of S1 results in the depletion of polysomes, accumulation of monosomes, and changes in the degradation rates of several mRNAs (37), which underscores the importance of S1 in regulating the interactions in the polysome. Recent cryo-EM data suggest that

S1 forms a wall of the tunnel between RNA-polymerase and the 30S subunit, consistent with its role in directing mRNAs onto the ribosome (38). Understanding of the exact role of protein S1 is challenging, because the structure of this six-domain protein on the ribosome is not available, and the current resolution of polysome structures is not high enough to make predictions (14, 38, 39). The 3D organization of polysomes, with neighboring 30S subunits facing each other, may allow protein S1 of the leading ribosome to hold the 5' end of the mRNA for the next ribosome. More structural information, e.g., a high-resolution structure of two adjacent ribosomes bound to the 5' leader, is required to solve this question.

In conclusion, our study provides a mechanistic insight into the initiation process during polysome assembly. Our results indicate the role of the initiation standby site during the ribosome loading on a polysome, explain the high TE of a highly translated mRNA, and suggests a mechanism for translational control in polysomes.

Materials and Methods

All experiments were carried out in buffer A (50 mM Tris-HCl, pH 7.5, 70 mM NH₄Cl, 30 mM KCl, 7 mM MgCl₂) at 37 °C. Stopped-flow experiments were performed using a SX-20MV apparatus (Applied Photophysics), mixing equal

volumes of 5**lpp* mRNA or 70S IC containing 5**lpp* mRNA (0.05 μM after mixing) with 30S PIC (0.4 or 0.05 μM after mixing) with or without the translation mixture (2 μM Phe-tRNA^{Phe} after mixing). For the natural *lpp* mRNA, equal volumes of 5**lpp-fl* or 70S IC with 5**lpp-fl* (0.15 μM) were mixed with the 30S PIC (0.5 μM). The Atto 488 fluorophore was excited at 465 nm, and the emission was monitored after passing through a KV500 cutoff filter. To measure the rate of poly(U) synthesis, the experiments were performed using a quench-flow apparatus (KinTek Laboratories, Inc.) by mixing equal volumes of the 70S IC and the translation mixture. The rate constants of 30S PIC recruitment to mRNA in a polysome were calculated by global fit of the deconvoluted time courses obtained at two concentrations of 30S PIC using KinTek Explorer (40). TE of *lpp* RBS was measured using dual luciferase reporter assay (SI Appendix).

ACKNOWLEDGMENTS. We thank Wolfgang Wintermeyer for critically reading the manuscript; Ingo Wohlgemuth, Henning Urlaub, and the facility for bioanalytical mass spectrometry for the comparative analysis of the ribosomal proteins in the WT and 70SΔ strain; Michael Pearson for the preparations of the 70SΔ ribosomes; and Olaf Geintzer, Sandra Kappler, Christina Kothe, Anna Pfeifer, Theresia Uhlendorf, Tanja Wiles, Franziska Hummel, and Michael Zimmermann for expert technical assistance. This work was supported by the Max Planck Society and by a grant from the Deutsche Forschungsgemeinschaft (FOR 1805).

- Gingold H, Pilpel Y (2011) Determinants of translation efficiency and accuracy. *Mol Syst Biol* 7:481.
- Plotkin JB, Kudla G (2011) Synonymous but not the same: The causes and consequences of codon bias. *Nat Rev Genet* 12:32–42.
- Li G-W (2015) How do bacteria tune translation efficiency? *Curr Opin Microbiol* 24:66–71.
- Espah Borujeni A, Channarasappa AS, Salis HM (2014) Translation rate is controlled by coupled trade-offs between site accessibility, selective RNA unfolding and sliding at upstream standby sites. *Nucleic Acids Res* 42:2646–2659.
- Farasat I, et al. (2014) Efficient search, mapping, and optimization of multi-protein genetic systems in diverse bacteria. *Mol Syst Biol* 10:731.
- Kudla G, Murray AW, Tollervey D, Plotkin JB (2009) Coding-sequence determinants of gene expression in *Escherichia coli*. *Science* 324:255–258.
- Proshkin S, Rahmouni AR, Mironov A, Nudler E (2010) Cooperation between translating ribosomes and RNA polymerase in transcription elongation. *Science* 328:504–508.
- Landick R, Carey J, Yanofsky C (1985) Translation activates the paused transcription complex and restores transcription of the *trp* operon leader region. *Proc Natl Acad Sci USA* 82:4663–4667.
- Kohler R, Mooney RA, Mills DJ, Landick R, Cramer P (2017) Architecture of a transcribing-translating expressome. *Science* 356:194–197.
- Mitarai N, Sneppen K, Pedersen S (2008) Ribosome collisions and translation efficiency: Optimization by codon usage and mRNA destabilization. *J Mol Biol* 382:236–245.
- Sørensen MA, Pedersen S (1991) Absolute in vivo translation rates of individual codons in *Escherichia coli*. The two glutamic acid codons GAA and GAG are translated with a threefold difference in rate. *J Mol Biol* 222:265–280.
- Jacobson LA, Baldassare JC (1976) Association of messenger ribonucleic acid with 70S monosomes from down-shifted *Escherichia coli*. *J Bacteriol* 127:637–643.
- Siwiak M, Zielenkiewicz P (2013) Transimulation: Protein biosynthesis web service. *PLoS One* 8:e73943.
- Brandt F, et al. (2009) The native 3D organization of bacterial polysomes. *Cell* 136:261–271.
- Kierzek AM, Zaim J, Zielenkiewicz P (2001) The effect of transcription and translation initiation frequencies on the stochastic fluctuations in prokaryotic gene expression. *J Biol Chem* 276:8165–8172.
- Kennell D, Riezman H (1977) Transcription and translation initiation frequencies of the *Escherichia coli* lac operon. *J Mol Biol* 114:1–21.
- Espah Borujeni A, Salis HM (2016) Translation initiation is controlled by RNA folding kinetics via a ribosome drafting mechanism. *J Am Chem Soc* 138:7016–7023.
- Tuller T, et al. (2010) An evolutionarily conserved mechanism for controlling the efficiency of protein translation. *Cell* 141:344–354.
- Chu D, et al. (2014) Translation elongation can control translation initiation on eukaryotic mRNAs. *EMBO J* 33:21–34.
- Milón P, Maracci C, Filonava L, Gualerzi CO, Rodnina MV (2012) Real-time assembly landscape of bacterial 30S translation initiation complex. *Nat Struct Mol Biol* 19:609–615.
- Studer SM, Joseph S (2006) Unfolding of mRNA secondary structure by the bacterial translation initiation complex. *Mol Cell* 22:105–115.
- La Teana A, Gualerzi CO, Brimacombe R (1995) From stand-by to decoding site. Adjustment of the mRNA on the 30S ribosomal subunit under the influence of the initiation factors. *RNA* 1:772–782.
- de Smit MH, van Duin J (2003) Translational standby sites: How ribosomes may deal with the rapid folding kinetics of mRNA. *J Mol Biol* 331:737–743.
- Sterk M, Romilly C, Wagner EGH (2018) Unstructured 5'-tails act through ribosome standby to override inhibitory structure at ribosome binding sites. *Nucleic Acids Res*, 10.1093/nar/gky073.
- Marzi S, et al. (2007) Structured mRNAs regulate translation initiation by binding to the platform of the ribosome. *Cell* 130:1019–1031.
- Duval M, et al. (2013) *Escherichia coli* ribosomal protein S1 unfolds structured mRNAs onto the ribosome for active translation initiation. *PLoS Biol* 11:e1001731.
- Goyal A, Belardinelli R, Maracci C, Milón P, Rodnina MV (2015) Directional transition from initiation to elongation in bacterial translation. *Nucleic Acids Res* 43:10700–10712.
- Braun V (1975) Covalent lipoprotein from the outer membrane of *Escherichia coli*. *Biochim Biophys Acta* 415:335–377.
- Li GW, Burkhardt D, Gross C, Weissman JS (2014) Quantifying absolute protein synthesis rates reveals principles underlying allocation of cellular resources. *Cell* 157:624–635.
- Neilsen PO, Zimmerman GA, McIntyre TM (2001) *Escherichia coli* Braun lipoprotein induces a lipopolysaccharide-like endotoxic response from primary human endothelial cells. *J Immunol* 167:5231–5239.
- Torti SV, Park JT (1976) Lipoprotein of gram-negative bacteria is essential for growth and division. *Nature* 263:323–326.
- Hirashima A, Childs G, Inouye M (1973) Differential inhibitory effects of antibiotics on the biosynthesis of envelope proteins of *Escherichia coli*. *J Mol Biol* 79:373–389.
- Nakamura K, Pirtle RM, Pirtle IL, Takeishi K, Inouye M (1980) Messenger ribonucleic acid of the lipoprotein of the *Escherichia coli* outer membrane. II. The complete nucleotide sequence. *J Biol Chem* 255:210–216.
- Kosuri S, et al. (2013) Composability of regulatory sequences controlling transcription and translation in *Escherichia coli*. *Proc Natl Acad Sci USA* 110:14024–14029.
- Kwak JE, Wickens M (2007) A family of poly(U) polymerases. *RNA* 13:860–867.
- Milón P, Konevega AL, Gualerzi CO, Rodnina MV (2008) Kinetic checkpoint at a late step in translation initiation. *Mol Cell* 30:712–720.
- Delvillani F, Papiani G, Dehò G, Briani F (2011) S1 ribosomal protein and the interplay between translation and mRNA decay. *Nucleic Acids Res* 39:7702–7715.
- Demo G, et al. (2017) Structure of RNA polymerase bound to ribosomal 30S subunit. *eLife* 6, 10.7554/eLife.28560.
- Byrgazov K, et al. (2015) Structural basis for the interaction of protein S1 with the *Escherichia coli* ribosome. *Nucleic Acids Res* 43:661–673.
- Johnson KA (2009) Fitting enzyme kinetic data with KinTek global kinetic explorer. *Methods Enzymol* 467:601–626.